Best Available Copy

64-12

ERR-FW-104
15 April 1964

HEAT TRANSFER IN HONEYCOMB SANDWICH PANELS

Published and distributed under Contract No. AF33(657)-11214, Air Force Materials Laboratory, Aeronautical Systems Division, Air Force Systems Command, Wright-Patterson Air Force Base, Ohio.

GENERAL DYNAMICS | FORT WORTH

ERR-FW-104
Aerothermodynamics

HEAT TRANSFER IN HONEYCOMB SANDWICH PANELS

J. V. CLIFTON

1 NOVEMBER 1961

ENGINEERING DEPARTMENT

This work was supported under General Dynamics/Fort Worth-sponsored research program Number 14-60-523.

GENERAL DYNAMICS | FORT WORTH

SUMMARY

Accurate analytical methods are presented for predicting the heat transfer and resulting temperature distribution in both brazed and bonded honeycomb sandwich panels during transient and steady state conditions. This analysis includes the heat transfer due to conduction through the cell walls as well as the heat exchange due to radiation within the cell. Heat transfer by convection is negligible.

An experimental investigation was conducted in which one surface of a honeycomb sandwich panel was heated by means of quartz radiant heaters and the resulting transient temperatures of the panel skins were measured and recorded. The test specimens consisted of brazed steel, brazed titanium and bonded aluminum panels, each having a thickness of approximately 1/2 inch. Excellent agreement between the experimental measurements and the analytical predictions have been obtained.

The results of the analytical and experimental investigations show that the heat transfer in the brazed panels is largely dependent on the thickness of brazing alloy which has accumulated on the cell walls during fabrication. Since the thermal conductivity of the brazing alloy, which is approximately 95% silver, is large (200 Btu/hr ft °F) compared to the conductivity of steel or titanium (10-14 Btu/hr ft °F), a very thin layer of brazing alloy on the cell wall can increase the heat transfer due to conduction through the core by a factor of 1 to 5 depending on the core geometry and amount of brazing alloy used per skin. For the 1/2 inch brazed panels considered in this study, the heat transfer due to conduction in the cell walls was increased by a factor of 3.08 and 2.4 due to the brazing alloy in the steel and titanium panels, respectively.

A significant parameter in the transfer of heat through bonded sandwich panels is the thermal resistance of the bonding material between the skins and core. The bonding material consists of one layer of glass cloth impregnated with phenolic resin. For the 1/2 inch bonded aluminum panel which was investigated during this study, the overall conductance of the core alone was calculated to be 46.7 Btu/hr ft^2 °F whereas the overall conductance of the bonded panel (core and bonding material) was calculated to be 3.03 Btu/hr ft^2 °F.

An effective or overall thermal conductivity has been predicted for each of the honeycomb panels (steel, titanium and aluminum). This effective thermal conductivity accounts for the heat exchange within the cell due to radiation as well as the conduction of heat through the cell walls. For the panels considered in this study the heat transfer due to convection and conduction within the air contained in the cells is negligible compared to conduction in the cell walls and radiation within the cells. The effect of heat exchange due to radiation within the cell can significantly increase the overall conductance of a given panel, depending on the temperature of the inner and outer skins, the cell wall emissivity and cell geometry.

TABLE OF CONTENTS

LIST OF FIGURES

LIST OF TABLES

NOMENCLATURE

Symbol	Description	Dimensions
a	cross sectional area of one cell	in^2
c	heat capacity	Btu/lb ^oF
F	radiation configuration factor	dimensionless
h	honeycomb core depth	in.
k	thermal conductivity	Btu/hr-ft-^oF
P	perimeter of cell wall	in.
t	time	sec.
T	temperature	^oR
x	coordinate	in.
α	one-half cell wall thickness	in.
β	braze alloy thickness on cell wall	in.
γ	cell wall thickness (2α)	in.
δ	inner skin thickness	in.
ϵ	emissivity	
ξ	dummy variable	
η	braze alloy thickness on inner skin	in.
ρ	density	lb/ft^3
σ	Stefan-Boltzmann's constant 0.174×10^{-8}	Btu/hr-ft^2-$^oR^4$
w	bonding material thickness between skin and core	in.

NOMENCLATURE
(Continued)

Subscripts

b	braze alloy or bonding material
c	core
e	effective
i	insulation or point within insulation
j	point within honeycomb core
o	outside or exposed skin
m	base metal of core (steel, titanium or aluminum)

1. INTRODUCTION

Honeycomb sandwich panels are currently being used in the construction of high performance aircraft and missiles and are also being proposed for construction of future high speed vehicles. The design of a vehicle for high speed flight must be supported by structural temperature predictions and the amount of heat transferred through the exterior panels during flight. In order to predict these quantities, it is necessary to have a knowledge of the heat transfer characteristics of the honeycomb panel.

Heat is transferred through the honeycomb core by means of (1) conduction in the cell walls, (2) conduction and convection in the air contained within the cells and (3) radiation within the cells. In order to simplify heat transfer calculations, it would be most desirable to consider the honeycomb core as a homogeneous medium which has a given specific heat, density, and some effective thermal conductivity which accounts for the combined effects of conduction, convection, and radiation heat transfer within the cell. Usually, the effective thermal conductivity of a given sandwich panel is obtained from experimental measurements during conditions of steady state heat transfer. However, the use of these experimental results for heat transfer predictions is limited to panels which are similar to the test specimens and also to design conditions within the range of test conditions. Since it is impractical to obtain extensive test data describing the heat transfer characteristics of all honeycomb sandwich panels of interest during various conditions of steady state and transient heat transfer, it is desirable to have an analytical method for predicting the heat transfer in these panels.

The purpose of this report is (1) to present an analytical method for predicting the heat transfer and resulting temperature distribution in both the brazed and bonded honeycomb sandwich panels during steady state and transient conditions and (2) to present an analytical method for predicting the effective thermal conductivity of honeycomb sandwich panels. The validity of the analytical method for predicting heat transfer in sandwich panels is supported by experimental measurements.

2. METHOD OF ANALYSIS

In general, the heat transfer in honeycomb sandwich panels is a result of (1) conduction of heat in the cell walls, (2) radiation interchange within the cell, and (3) convection and/or conduction of heat through the air contained in the cell. However, this report is concerned with sandwich panels in which the primary modes of heat transfer are due to conduction in the cell walls and radiation exchange within the cell. For most honeycomb cores used in the fabrication of sandwich panels (core density from 4 to 12 lb/ft^3), it can be shown that the heat exchange by convection and conduction within the air contained in the cell is negligible compared to conduction in the cell walls and radiation within the cell.

This section of the report will present the general heat transfer analysis of (1) a typical brazed panel, (2) a typical bonded panel and (3) the effective thermal conductivity of honeycomb cores. The boundary conditions (heat transfer at inner and outer skins) imposed on the equations which describe the heat transfer in the honeycomb sandwich panels will be consistent with the boundary conditions of the experimental investigation so that a comparison of theory and experimental results is possible.

2.1 Brazed Panel

A brazed sandwich panel is one in which the skins are attached to the honeycomb core by means of a brazing alloy. The sandwich panel skins and core are usually steel or titanium while the brazing alloys in common use today contain over 95% silver. This alloy is uniformly applied to both skins between the skins and core. The panel is then placed horizontally and heated to a temperature of approximately 1600°F such that the braze alloy will become soft and flow, forming a metallic bond between the skins and core upon cooling.

Previous efforts to determine the effective thermal conductivity of brazed honeycomb sandwich panels from experimental measurements have shown the effective thermal conductivity of the core, at low temperature where radiation interchange within

the cell is unimportant, to be greater than the predicted values based on conduction through the cell wall and the air contained in the cell. A visual observation of a panel cross-section shows that a small amount of silver brazing collected on the cell walls during the brazing process. Since the thermal conductivity of silver is high (approximately 200 Btu/hr-ft-^{o}F), compared to steel or titanium, a very small amount of silver brazing alloy on the cell walls will significantly increase the amount of heat transfer through the panel due to conduction. A brief analysis shows good agreement between the heat transfer measurements and predictions at low temperatures assuming a small percent of the brazing alloy on one skin is uniformly distributed on the cell walls. In the following analysis, it will be assumed that a uniform thickness of silver brazing alloy is distributed on the cell walls.

For convenience, consider a single cell of a honeycomb core as shown in Figure 1, with inner and outer skins attached. An energy balance across the increment of Δx thickness gives the following equation which describes the heat transfer and temperature distribution within the core:

$$\left[(\rho c)_m \alpha + (\rho c)_b \beta\right] P \Delta x \frac{\partial T}{\partial x}(x,t) = \left[k_m \alpha + k_b \beta\right] P \left[\frac{\partial T}{\partial x}(x,t) - \frac{\partial T}{\partial x}(x+\Delta x,t)\right] +$$

$$+ \sigma \epsilon P \Delta x \left\{ \int_0^x f_1(x,\xi)\left[T(\xi,t)^4 - T(x,t)^4\right] d\xi - \int_{x+\Delta x}^h f_1(x,\xi)\left[T(x,t)^4 - T(\xi,t)^4\right] d\xi + \right.$$

$$\left. + f_2(x)\left[T(0,t)^4 - T(x,t)^4\right] + f_3(x)\left[T(h,t)^4 - T(x,t)^4\right] \right\}, \quad 0 \le x \le h \qquad (1)$$

where the function $f_1(x,\xi)$ describes the radiation configuration factor between the increment Δx at the point x and any other point ξ within the cell. The functions $f_2(x)$ and $f_3(x)$ describe the configuration factor between the increment and the outer and inner skins respectively. The quantity $\frac{\partial T}{\partial x}(x+\Delta x,t)$ can be expressed in terms of the point x by expansion in a Taylor series, as follows:

The functions $f_4(h,\xi)$ and $f_5(0)$ describe the configuration between inner skin ($x=h$) and any point ξ within the cell and the outer skin ($x=0$) respectively. The quantity $k_1 a \frac{\partial T_1}{\partial x}(h,t)$ is the heat transferred by conduction from the inner skin to the back-up insulation. In order for the above equations which describe the heat transfer at the inner boundary of brazed honeycomb sandwich panels to be consistent with the experimental conditions, the heat transfer between the inner skin and the back-up insulation must be considered (See Section 3). The heat transfer in the insulation is described by

$$(\rho c)_i \frac{\partial T_i}{\partial t}(x,t) = k_i \frac{\partial^2 T_i}{\partial x^2}(x,t), \quad h \le x \le L, \tag{7}$$

with the following boundary conditions

$$T(h,t) = T_1(h,t), \quad x = h, \tag{8}$$

and

$$\frac{\partial T_1}{\partial x}(L,t) = 0, \quad x = L, \tag{9}$$

Equations (3) through (9) describe the heat transfer within the cell and insulation and define the temperature at any point within the cell and insulation for a given initial temperature and any variation of outer skin temperature with respect to time. Since there is no exact analytical solutions for the above set of equations, a finite difference method of solution will be used. Since these equations describe the heat transfer throughout the sandwich panel and insulation, they also describe the heat transfer and define the temperature at any given point or increment in the sandwich panel or insulation within the range of restrictions on each equation. Therefore the eqations defining the temperature at any point j in the cell and any point i in the insulation can be written as follows:

$$\frac{\partial T_j}{\partial t} = A\frac{\partial^2 T_j}{\partial x^2} + B\left\{\int_0^h f_1(x,\xi)\left[T(\xi,t)^4 - T_j^4\right]d\xi + \right.$$

$$\left. + f_2(x)\left[T(0,t)^4 - T_j^4\right] + f_3(x)\left[T(h,t)^4 - T_j^4\right]\right\}, \; 0 \le x \le h, \qquad (10)$$

$$\frac{\partial T_j}{\partial t} = \frac{\partial T_i}{\partial t} = C\frac{\partial T_j}{\partial x} - D\frac{\partial T_i}{\partial x} + E\left\{\int_0^h f_4(h,\xi)\left[T(\xi,t)^4 - T_j^4\right]d\xi + \right.$$

$$\left. + f_5(0)\left[T(0,t)^4 - T_j^4\right]\right\}, \; x = h, \qquad (11)$$

$$\frac{\partial T_i}{\partial t} = G\frac{\partial^2 T_i}{\partial x^2}, \qquad h \le x \le L, \qquad (12)$$

$$\frac{\partial T_i}{\partial x} = 0, \quad x = L, \qquad (13)$$

where the coefficients A, B, C, D, E and G are defined as

$$A = \frac{k_m\alpha + k_b\beta}{(\rho c)_m\alpha + (\rho c)_b\beta}$$

$$B = \frac{\sigma\epsilon}{(\rho c)_m\alpha + (\rho c)_b\beta}$$

$$C = \frac{[k_m\alpha + k_b\beta]P}{[(\rho c)_m\alpha + (\rho c)_b\beta]a}$$

$$D = \frac{k_l}{(\rho c)_m\delta + (\rho c)_b\eta}$$

$$E = \frac{\sigma\epsilon}{(\rho c)_m\delta + (\rho c)_b\eta}$$

and

$$G = \frac{k_i}{(\rho c)_i}$$

The partial derivatives can be expressed in finite difference form as

$$\frac{\partial T_j}{\partial x} = \frac{T_{j-1} - T_{j+1}}{2\Delta x_j} \tag{14}$$

and

$$\frac{\partial^2 T_j}{\partial x^2} = \frac{T_{j-1} + T_{j+1} - 2T_j}{(\Delta x)^2} \tag{15}$$

Substitution of equations (14) and (15) in equations (10) thru (13) results in

$$\frac{\partial T_j}{\partial t} = A\left[\frac{T_{j+1} + T_{j-1} - 2T_j}{(\Delta x_j)^2}\right] + B\sum_{n=0}^{p} F_{j-n}\left[T_n^4 - T_j^4\right], \quad 0 \le x \le h \tag{16}$$

$$\frac{\partial T_j}{\partial t} = C\left[\frac{T_{j-1} - T_{j+1}}{2\Delta x_j}\right] - D\left[\frac{T_{i-1} - T_{i+1}}{2\Delta x_i}\right] + E\sum_{n=0}^{p} F_{j-n}\left[T_n^4 - T_j^4\right], \quad x = h \tag{17}$$

$$\frac{\partial T_i}{\partial t} = G\left[\frac{T_{i+1} + T_{i-1} - 2T_i}{(\Delta x_i)^2}\right], \quad h \le x \le L \tag{18}$$

$$\frac{T_{i-1} - T_{i+1}}{2\Delta x_i} = 0, \quad x = L \tag{19}$$

At the inner skin (x=h), equations (16), (17), and (18) must be solved simultaneously for the quantity $\frac{\partial T_j}{\partial t}(h,t)$, since the temperatures T_{j+1} and T_{i-1} in these equations are not defined at the point x = h. Therefore, solving for T_{j+1} and T_{i-1} in equations

(16) and (18) respectively and substituting into equation (17) gives the quantity $\frac{\partial T_j}{\partial t}$ (h,t) in terms of known temperatures T_{j-1} and T_{i+1}.

$$\frac{\partial T_j}{\partial t} = H(T_{j-1} - T_j) - J(T_i - T_{i-1}) + K\sum_{n=0}^{p} F_{j-n}\left(T_n^4 - T_j^4\right), \quad x = h \qquad (20)$$

where the coefficient H, J, and K are defined as

$$H = \frac{k_m\left[1 + k_b\beta / k_m\alpha\right]}{\Delta x_j\left[\frac{a}{P\alpha}\right]\left\{\left[(\rho c)_m\delta + (\rho c)_b\eta\right] + \frac{P\Delta x_i}{2a}\left[(\rho c)_m\alpha + (\rho c)_b\beta\right] + \frac{(\rho c)_i\Delta x_i}{2}\right\}}$$

$$J = \frac{k_i}{\Delta x_i\left\{\left[(\rho c)_m\delta + (\rho c)_b\eta\right] + \frac{P\Delta x_i}{2a}\left[(\rho c)_m\alpha + (\rho c)_b\beta\right] + \frac{(\rho c)_i\Delta x_i}{2}\right\}}$$

and

$$K = \frac{\sigma\epsilon\left[\frac{P\Delta x_i}{a} + 1\right]}{\left\{\left[(\rho c)_m\delta + (\rho c)_b\eta\right] + \frac{P\Delta x_i}{2a}\left[(\rho c)_m\alpha + (\rho c)_b\beta\right] + \frac{(\rho c)_i\Delta x_i}{2}\right\}}$$

At the inner surface of the insulation (x=L) equations (18) and (19) must be solved simultaneously to eliminate the temperature T_{i+1}, since this temperature does not exist at x = L. Since $T_{i-1} = T_{i+1}$ at x = L equations (18) and (19) become

$$\frac{\partial T_i}{\partial t}(L,t) = \frac{2G(T_{i-1} - T_i)}{(\Delta x)_i^2}, \quad x = L \qquad (21)$$

The finite difference equations which describe the temperature distribution within a brazed honeycomb sandwich panel are summarized below for the conditions in which (1) the outer skin temperature is known to vary with respect to time in any arbitrary manner and (2) heat is transferred from the inner skin by conduction to a medium having different thermal properties.

$$T_j = T_o(t), \qquad x = 0 \text{ or } j = 0 \qquad (5)$$

$$\frac{\partial T_j}{\partial t} = A\left[\frac{T_{j+1} + T_{j-1} - 2T_j}{(\Delta x_j)^2}\right] + B\sum_{n=0}^{p} F_{j-n}\left[T_n^4 - T_j^4\right], j = 1, 2, \cdots, p, \quad (16)$$

$$\frac{\partial T_j}{\partial t} = H(T_{j-1} - T_j) - J(T_i - T_{i+1}) + K\sum_{1} F_{j-n}(T_n^4 - T_j^4), \quad (20)$$

where $T_j = T_i$, $x = h$ or $j = i = p$

$$\frac{\partial T_i}{\partial t} = G\left[\frac{T_{i+1} + T_{i-1} - 2T_i}{(\Delta x_i)^2}\right], i = p+1, p+2, \cdots, g \quad (18)$$

$$\frac{\partial T_i}{\partial t} = 2G\left[\frac{T_{i-1} - T_i}{(\Delta x_i)^2}\right], i = g \text{ or } x = L \quad (21)$$

These equations have been set-up for solution on an electronic analog computer.

2.2 Bonded Panels

A bonded sandwich panel is one in which the skins are bonded to the honeycomb core by means of an adhesive bonding material. This bonding material is normally one sheet of glass cloth impregnated with a phenolic resin.

A significant factor in the transfer of heat through bonded panels is the thermal resistance provided by the adhesive bonding material between the skins and core. A heat transfer model of the bonded panel is shown in Figure 2. Using a technique similar to that of the previous section, the equations which describe the heat transfer in bonded panels can be developed and are presented as follows:

$$\frac{\partial T_j}{\partial t} = A'(T_0 - T_j) - B'(T_j - T_{j+1}) + C'\sum_{n=0}^{p} F_{j-n}(T_n^4 - T_j^4), j = 1, \quad (22)$$

$$\frac{\partial T_j}{\partial t} = D'(T_{j-1}+T_{j+1}-2T_j) + E'\sum_{n=0}^{p-1} F_{j-n}(T_n^4 - T_j^4), \; j=2,3,\cdots,p-2 \quad (23)$$

$$\frac{\partial T_j}{\partial t} = B'(T_{j-1}-T_j) - A'(T_j - T_{j+1}) + C'\sum_{n=0}^{p-1} F_{j-n}(T_n^4 - T_j^4), \; j=p-1, \quad (24)$$

$$\frac{\partial T_j}{\partial t} = G'(T_{j-1}-T_j) - H'(T_i - T_{i+1}), \; i=j=p, \quad (25)$$

$$\frac{\partial T_i}{\partial t} = J'(T_{i-1}+T_{i+1}-2T_i), \; i=p+1, p+2, \cdots, g-1, \quad (26)$$

$$\frac{\partial T_i}{\partial t} = K'(T_{i-1}-T_i), \quad i=g, \quad (27)$$

where

$$A' = \frac{2k_b a}{(\rho c)_m p\alpha w \Delta x_j} \qquad K' = \frac{2k_i}{(\rho c)_i (\Delta x_i)^2}$$

$$B' = \frac{2k_m}{(\rho c)_m (\Delta x_j)^2}$$

$$C' = \frac{2\sigma\epsilon a}{(\rho c)_m \Delta x_j \, p\alpha}$$

$$D' = \frac{k_m}{(\rho c)_m (\Delta x_j)^2}$$

$$E' = \frac{\sigma\epsilon}{(\rho c)_m \alpha}$$

$$G' = \frac{k_b}{[(\rho c)_b w + (\rho c)_m \delta + (\rho c)_i \Delta x_i/2] w}$$

$$H' = \frac{k_i}{\left[(\rho c)_b \omega + (\rho c)_m \delta + (\rho c)_i \, \Delta x_i/2\right] \Delta x_i}$$

$$J' = \frac{k_i}{(\rho c)_i (\Delta x_i)^2}$$

Equations (22) through (27) have been set-up for solution on an electronic analog computer.

2.3 Effective Thermal Conductivity of Core

The effective thermal conductivity "$k_e(T)$" of a honeycomb core will be defined in the following statements. In Figure 1, the total amount of heat passing the point x in the core at any time t can be expressed as

$$k_e(T) a \frac{\partial T}{\partial x}(x,t) = (k_m \alpha + k_b \theta) P \frac{\partial T}{\partial x}(x,t) + \sigma \epsilon a \Big\{ \Big\{ \int_0^h f_6(x,\xi)\left[T(\xi,t)^4 - T(x,t)^4\right] d\xi + + f_7(x)\left[T(0,t)^4 - T(x,t)^4\right] - f_8(x)\left[T(x,t)^4 - T(h,t)^4\right]\Big\}, \quad (28)$$

where $f_6(x,\xi)$, $f_7(x)$ and $f_8(x)$ are the configuration factors between the area "a" at the point "x" and the cell walls, the outer skin (x=0), and the inner skin (x=h) respectively. Solving for $k_e(T)$ in equation (28) gives

$$k_e(T) = (k_m \alpha + k_b \theta) P/a + \sigma \epsilon \Big/ \frac{\partial T}{\partial x}(x,t) \Big\{ \int_0^h f_6(x,\xi)\left[T(\xi,t)^4 - T(x,t)^4\right] d\xi + f_7(x)\left[T(0,t)^4 - T(x,t)^4\right] + - f_8(x)\left[T(x,t)^4 - T(h,t)^4\right], \quad (29)$$

Thus, the effective thermal conductivity of a honeycomb core is a function of the conductivity of the cell walls including both the core metal and brazing alloy* plus a complex function of the cell geometry and temperature distribution through the cell. Therefore, for a given hon yoomb core, there exists an infinite number of values for the effective thermal conductivity, depending entirely on the temperature distribution through the cell, i.e. $k_e(T)$ is not a single valued function of temperature.

Although, $k_e(T)$ cannot, in general, be expressed as a single valued function of temperature, it is possible that an effective thermal conductivity can be defined for certain limiting conditions. The most convenient condition, is that of steady state heat transfer through a cell in which the temperature distribution through the cell will be similar for any combination of outer and inner skin temperatures. Then for steady state heat transfer through a honeycomb core, the function $k_e(T)$ can be expressed in terms of the average core temperature for a given temperature difference across the core as illustrated in Figure 3.

For steady state conditions, equation (28) is most easily evaluated at $x = h$ and is expressed as

$$k_e a\left[T(0)-T(h)\right]/h = \left(k_m\alpha + k_b\beta\right)p\frac{\partial T}{\partial x}(h) +$$

$$+\sigma\epsilon a\left\{\int_0^h f_6(h,\xi)\left[T(\xi)^4-T(h)^4\right]+f_7(0)\left[T(0)^4-T(h)^4\right]\right\} \quad (30)$$

or in finite difference form after simplification.

*For the case of bonded panels, $\beta = 0$

$$(k_e/k_m)(1+k_b\beta/k_m\alpha)^{-1}(P\alpha/a)^{-1} = (h/\Delta x)\left[(T_{p-1}-T_p)/(T_o-T_p)\right] +$$

$$+ \frac{\sigma\epsilon h a}{k_m P\alpha[T(o)-T(h)]}(1+k_b\beta/k_m\alpha)^{-1}\sum_{n=o}^{p-1} F_{p-n}(T_n^4 - T_p^4)\,, \qquad (31)$$

The quantity $a/P\alpha$ can be replaced by the ratio of core metal density to overall core density ρ_m/ρ_c for convenience. In section 4.2.1, the effective thermal conductivities for the brazed steel, brazed titanium and bonded aluminum panels are given.

In regard to transient heat transfer within a honeycomb core, a few of the limiting conditions for which an effective thermal conductivity can be defined are listed as follows:

(a) heat transfer in the cell is primarily a result of conduction and the temperature distribution through the cell is essentially linear

(b) heat transfer in the cell is primarily due to radiation between the skins, in which case the temperature distribution through the cell is not important

(c) for small time rate of change of outer and inner skin temperatures such that temperature distribution within the cell remains similar with respect to inner and outer skin temperatures. This represents the case of a core with zero or small heat capacity $(\rho c)_c h$ with respect to the skins $(\rho c)_m \delta$, i.e. a quasi-steady state temperature distribution within the core exists.

3. TEST DESCRIPTION

The honeycomb sandwich panel test specimens which were used in this study were cut from production panels which were fabricated by Convair Fort Worth. These specimens consisted of one brazed steel, one brazed titanium and one bonded aluminum panel. A typical test specimen is illustrated in Figure 4. A description of each test specimen is given in Table 1.

In the case of the brazed panels, the outer and inner skins are brazed to the core with approximately 0.106 lb of silver brazing alloy per square foot of skin area. The aluminum skins are bonded to the aluminum core by means of a single layer of glass cloth impregnated with phenolic resin and placed between the skins and core.

Thermocouples (No. 30 gage chromel-alumel) were attached to the inner and outer skins of the panel as shown in Figure 4. The temperatures measured by the thermocouples were recorded with an oscillograph.

The test specimens were heated by means of a quartz radiant heater as illustrated in Figure 5. The energy incident on the specimens was controlled by regulating the electrical power supplied to the quartz heater. Each specimen was placed horizontally on piece of fiberfrax thermal insulating material as shown in Figure 5, and exposed to three heating rates such that the time rate of change of exposed skin temperature was approximately 40, 80 and 120 °F per sec. For each heating condition, the initial temperature was constant through the panel and insulation.

TABLE 1. DESCRIPTION OF TEST SPECIMENS

	Brazed Steel	Brazed Titanium	Bonded Aluminum
outer skin thickness-in.	0.010	0.022	0.014
inner skin thickness-in.	0.008	0.022	0.034
core depth-in.	0.614	0.505	0.631
core density-lb/ft^3	8.4	10.48	6.1
cell size-in.	0.1875 sq.	0.1875 sq.	0.125 hex.
cell wall thickness-in.	0.00165	0.00354	0.0017
skin material	steel	titanium	aluminum
core material	steel	titanium	aluminum

4. DISCUSSION OF RESULTS

4.1 Comparison of Predictions with Measurements

A comparison of the analytical predictions of heat transfer in honeycomb sandwich panels with experimental measurements, are presented and discussed in this section of the report. For each test specimen, the solution of the equations in Section 2.2 or 2.3 for the inner skin temperature will be compared with the corresponding values of measured temperature for a given outer skin temperature.

4.1.1 Brazed Steel Panel

The thermal properties of the steel panel, required for evaluation of the coefficients A, B, G, J, and K are listed below:

$k_m = 10.4$ Btu/hr ft ^oF, $k_b = 210$

$\rho_m = 477$ lb/ft^3 , $\rho_b = 656$

$C_m = 0.13$ Btu/lb ^oF , $C_b = 0.06$

$\alpha = \gamma/2 = 8.27 \times 10^{-4}$ in, $\eta = 0.00194$ in.

$\delta = 0.008$ in. , $P = 0.75$ in.

$\epsilon = 0.8$, $\Delta x_j = 0.123$ in.

$\Delta x_i = 0.05$ in. , $\rho_i = 10.6$ lb/ft^3

$C_i = 0.20$ Btu/lb ^oF , $k_i = 0.025$ Btu/hr ft ^oF

$a = 0.0352$ sq. in.

A total of six nodes (p=5) have been selected within the brazed steel panel. The radiation configuration factors between any given node and all other nodes are given in Table 2.

TABLE 2. CONFIGURATION FACTORS "F_{j-n}" FOR BRAZED STEEL PANEL

BRAZED STEEL PANEL

CORE DEPTH - 0.614 INCH
CELL SIZE - 3/16 INCH SQUARE CELL

	j					
n	0	1	2	3	4	5
0		0.2705	0.0678	0.0217	0.0090	0.0340
1	0.7080		0.2027	0.0461	0.0127	0.0235
2	0.1777	0.2027		0.2027	0.0461	0.0568
3	0.0568	0.0461	0.2027		0.2027	0.1777
4	0.0235	0.0127	0.0461	0.2027		0.7080
5	0.0340	0.0090	0.0217	0.0678	0.2705	

Since the average thickness of brazing alloy (β) which has accumulated on the cell walls. is not known, the coefficients A, B, G, H, J, and K will be expressed in terms of β and are listed below

$$A = 0.484\left[\frac{1+24400}{1+833\beta}\right]$$

$$B = 1.22\times10^{-10}\left[\frac{1}{1+833\beta}\right]\epsilon$$

$$H = 0.115\left[\frac{1+22400}{1.249+99.3\beta}\right] \quad \text{for } \eta = 0.00194 \text{ in.}$$

$$J = \frac{0.00461}{(1.249+99.3\beta)} \quad \text{for } \eta = 0.00194 \text{ in.}$$

$$K = \frac{1.11\times10^{-11}\epsilon}{(1.249+99.3\beta)} \quad \text{for } \eta = 0.00194 \text{ in.}$$

$$G = 0.1886$$

$$0 \le \beta \le 18\times10^{-5} \text{ in.}$$

Equations (16), (18), (20) and (21) have been solved with the aid of an electronic analog computer for various values of β. The values of β have been selected within the limits

$$0 \le \beta \le \beta_{max}$$

where β_{max} is the thickness of brazing alloy on the cell walls if all the alloy from one skin was uniformly distributed on the cell walls. The correct value of β is assumed to be that which results in agreement between predicted and measured inner skin temperature for a given heating condition.

Figure 6 shows the effects of the brazing alloy and the cell wall emissivity on the inner skin temperature for a given heating condition. The value of β which results in agreement between theory and experimental measurements is 8.5×10^{-5} inches. Since this value of β also results in agreement between predicted and measured values of inner skin temperature for all three heating rates as shown in Figure 7, it is assumed that the average thickness of silver brazing alloy on the cell walls of the brazed steel panel is 8.5×10^{-5} inches.

This thickness of brazing alloy increases the heat transfer due to conduction through the cell walls by a factor of 3.08 compared to the heat transfer through the steel cell walls neglecting the brazing alloy. The heat capacity $(\rho C)_m$ of the cell wall alone is increased by a factor of 1.0654 due to the presence of the silver brazing alloy.

4.1.2 Titanium Brazed Panel

The thermal property data required to evaluate the coefficients A, B, G, H, J and K in equations (16), (18), (20) and (21) are listed below:

$k_m = 9$ Btu/hr ft $^{\circ}$F, $\quad k_b = 210$

$\rho_m = 283$ lb/ft^3 , $\quad \rho_b = 656$

$c_m = 0.14$ Btu/lb $^{\circ}$F, $\quad C_b = 0.06$

$\alpha = 0.00177$ in., $\quad \eta = 0.00194$ in.

$\Delta x_j = 0.101$ in., $\quad \Delta x_1 = 0.05$ in.

$\rho_1 = 10.6$ lb/ft^3, $\quad \delta = 0.022$ in.

$C_1 = 0.20$ Btu/lb $^{\circ}$F, $\quad \epsilon = 0.35$

$k_1 = 0.025$ Btu/hr ft $^{\circ}$F, P = 0.75 in.

$a = 0.0352$ in^2

With these constants, the coefficients A, B, G, H, J and K are evaluated in terms of the brazing alloy thickness on the cell wall

$$A = 0.892 \left[\frac{1+13200}{1+562\beta}\right]$$

$$B = 9.72x10^{-11} \left[\frac{1}{1+562\beta}\right]\epsilon$$

$$G = 0.1888$$

$$H = 0.1392 \left[\frac{1+1.32x10^{4}}{1.137+44.5\beta}\right] \quad \text{for } \eta = 0.00194 \text{ in.}$$

$$J = \frac{1.056x10^{-3}}{1.137+44.5\beta} \quad \text{for } \eta = 0.00194 \text{ in.}$$

$$K = 0.610x10^{-11} \left[\frac{1}{1.137+44.5\beta}\right]\epsilon$$

$$\text{for } \eta = 0.00194 \text{ in.}$$

$$0 \leq \beta \leq 18x10^{-5} \text{ in.}$$

A total of six nodes or five increments have also been selected for the finite difference solution of equations (16), (18), (20) and (21). The radiation configuration factors between any given node and all other nodes are given in Table 3.

Figure 8 shows the effect of the brazing alloy and the cell wall emissivity on the inner skin temperature for a given heating condition.

The value of β which caused the theory and experimental measurements to match is $9.0x10^{-5}$ inches. It is not surprising that the values of β for the steel brazed and titanium panels are approximately the same

TABLE 3. CONFIGURATION FACTORS "F_{j-n}" FOR BRAZED TITANIUM PANEL

BRAZED TITANIUM PANEL

CORE DEPTH - 0.505 INCH
CELL SIZE - 3/16 INCH SQUARE CELL

n \ j	0	1	2	3	4	5
0		0.3000	0.0954	0.0348	0.0153	0.0496
1	0.6400		0.2046	0.0606	0.0195	0.0327
2	0.2036	0.2046		0.2046	0.0606	0.0741
3	0.0741	0.0606	0.2046		0.2046	0.2036
4	0.0327	0.0195	0.0606	0.2046		0.6400
5	0.0496	0.0153	0.0348	0.0954	0.3000	

since the same amount of brazing alloy is used for each panel and both panels have the same cell geometry and core depth. Figure (9) gives the comparison of predicted and measured inner skin temperature for three different heating rates.

This thickness of brazing alloy increases the heat transfer due to conduction through the cell walls by a factor of 2.4 compared to the heat transfer through the cell walls neglecting the brazing alloy. The product of density and heat capacity of the titanium cell wall alone is increased by a factor of 1.0505 due to the presence of the silver brazing alloy.

4.1.3 Bonded Aluminum Panel

The thermal properties of the bonded aluminum panel, which are required for evaluation of the coefficients A', B', C', D', E', G', H', J' and K' in equations (22) through (27) are listed below

$k_m = 81$ Btu/hr ft $^{\circ}$F, $\quad k_b = 0.1$ Btu/hr ft $^{\circ}$F

$\rho_m = 168$ lb/ft^3, $\quad \rho_b = 120$ lb/ft^3

$C_m = 0.23$ Btu/lb $^{\circ}$F, $\quad C_b = 0.25$ Btu/lb $^{\circ}$F

$k_i = 0.025$ Btu/hr ft $^{\circ}$F, $\quad \alpha = 8.5\text{x}10^{-4}$ in.

$\rho_i = 10.6$ lb/ft^3, $\quad \delta = 0.034$ in.

$C_i = 0.20$ Btu/lb $^{\circ}$F, $\quad P = 0.51$ in.

$\Delta x_j = 0.1578$ in. $\quad \Delta x_i = 0.05$ in.

$\epsilon = 0.2$ $\quad a = 0.01354$ in^2

Since the average thickness of bonding material "w" between the skins and core is unknown, the coefficients which depend on w will be expressed in terms of w. The coefficients A' through E' and G' through K' are listed below for the bonded aluminum panel.

$$A' = \frac{0.0412}{w}$$

$$B' = 6.76$$

$$C' = 1.802 \times 10^{-10} \epsilon$$

$$D' = 3.38$$

$$E' = 1.768 \times 10^{-10} \epsilon$$

$$G' = \frac{0.002635}{w}$$

$$H' = 0.011$$

$$J' = 0.1887$$

$$K' = 0.3774$$

Four increments within the core plus the nodes representing each skin were used for the finite difference solution of the temperature distribution in the bonded aluminum panel. The radiation configuration factors between any node or increment and all other nodes are given in Table 4 for the aluminum panel.

Figure 10 shows the effect of the bonding material and cell wall emissivity on the inner skin temperature for a given outer skin temperature. The value of w which causes the theory and experimental measurements to agree is 0.0065 inches. Using this value of w, the predicted inner skin temperature for three different heating rates is compared in Figure 11 with experimental measurements.

The bonding material between the skins and core offers a significant increase in the thermal resistance of this panel. For this particular bonded aluminum panel, the overall conductance of the core alone was approximately 46.7 Btu/hr ft^2 °F whereas the overall conductance of the core and bonding material (0.0065 inches fiberglas) is 3.03 Btu/hr. ft^2 °F.

TABLE 4. CONFIGURATION FACTORS "F_{j-n}" FOR BONDED ALUMINUM PANEL

BONDED ALUMINUM PANEL

CORE DEPTH - 0.631 INCH
CELL SIZE - 1/8 INCH HEXAGONAL CELL

	j				
n	1	2	3	4	5
1		0.8213	0.1201	0.0309	0.0278
2	0.2114		0.1805	0.0230	0.0080
3	0.0309	1.1805		0.1805	0.0309
4	0.0080	0.0230	0.1805		0.2114
5	0.0278	0.0309	0.1201	0.8213	

In Figure 11, notice that the effect of radiation within the cell is almost negligible. A change in cell wall emissivity from zero to one produces a change in inner skin temperature of only 14°F for this heating condition. The negligible effect of radiation, is however expected, since the temperature level of the panel is relatively low and the cell size is small with a resulting small radiation configuration factors.

4.2 Effective Thermal Conductivity

Based on the method of analysis in Section 2.3.1 the effective thermal conductivities for the honeycomb cores of the brazed steel, the brazed titanium and the bonded aluminum panels considered in this study have been obtained. The $k_e(T)$ for each panel is based on steady state heat transfer through the sandwich panel. Figures 12 and 13 give the effective conductivities of the brazed steel and brazed titanium panels respectively as a function of average panel (or core) temperature for various temperature differences across the core. A comparison of the predicted and measured values of $k_e(T)$ was not possible, since experimental measurements of the steady state heat transfer through these panels is not available. However, these predictions of $k_e(T)$ are considered to be reasonably accurate since the steady state heat transfer calculations, from which $k_e(T)$ are obtained, is identical with the transient analysis for which excellent agreement between predicted and measured temperatures were obtained. This method for predicting $k_e(T)$ should be compared with experimental measurements of steady state heat transfer through a given sandwich panel for further verification.

Notice that $k_e(T)$ for the titanium core varies less with the average panel temperature than that of the steel core. This difference is due to (1) more heat being transferred by conduction in the titanium panel and (2) less heat being transferred by radiation within the titanium panel, as compared to the steel panel, for a given outer and inner skin temperature.

Calculations show that the effective thermal conductivity of the aluminum core does not vary significantly with temperature. This means that the heat transfer due to radiation within the aluminum core is negligible compared to the heat transfer by conduction. This is due to the low emissivity of aluminum (ϵ = 0.2) and the small radiation configuration factors within the cell (1/8 inch hexagonal cell). Therefore the effective thermal conductivity of the core is simply

$$k_e = k_m \frac{\rho_c}{\rho_m} \quad \text{or}$$

$$k_e = 2.94 \text{ Btu/hr ft } {}^{\circ}\text{F}$$

However an additional resistance to heat transfer through the panel is offered by 0.0065 inches of bonding material (fiberglas) between each skin and the core. The thermal properties of the bonding material is given in Section 4.1.3.

It is important to note that the effective thermal conductivities given in this section are valid only for the particular test specimens used in this study. The effective thermal conductivities of the steel and titanium cores given in Figures 12 and 13 should not be used for heat transfer predictions without further verification by additional experimental measurements. Honeycomb cores having different depth, different cell size or different cell wall thickness will have different overall thermal properties. Variations in fabrication techniques may result in a different amount of braze alloy collecting on cell walls of brazed panels or in a different thickness of bonding material between the core and skins of bonded panels.

5. CONCLUSIONS

(1) Accurate analytical methods have been developed and are presented in Section 2.1 and 2.2 for predicting the heat transfer and resulting temperature distribution in both brazed and bonded honeycomb sandwich panels. The significant parameters for consideration when predicting the heat transfer or temperature distribution in brazed or bonded panels are listed as follows.

   (a) thickness of brazing alloy which accumulates on the cell walls during fabrication of the brazed panels.

   (b) thickness of brazing alloy which remains on the panel skins during fabrication of the brazed panels

   (c) thickness of bonding material between the core and skins of bonded panels

   (d) cell wall emissivity of both brazed and bonded panels

   (e) cell wall thickness of both brazed and bonded panels

   (f) cell geometry for determining radiation configuration factors

(2) An analytical method for predicting the effective thermal conductivity of honeycomb cores has been developed and is presented in Section 2.3. In general, the effective thermal conductivity of a honeycomb core is shown to be a function of the conductivity of the cell walls including both the core metal and brazing alloy (for brazed panels only) plus a complex function of the cell geometry and temperature distribution through the cell.

6. RECOMMENDATIONS

(1) The analytical analysis presented in Section 2.1 and 2.2 should be used to accurately predict the heat transfer and temperature distribution in brazed and bonded honeycomb sandwich panels for both transient and steady state conditions.

(2) The method of analysis presented in Section 2.3 can be used to predict the effective thermal conductivity of honeycomb cores for conditions of steady state heat transfer.

(3) Although the effective thermal conductivity of honeycomb cores is defined for conditions of steady state heat transfer, it can also be used for purposes of preliminary calculations of transient heat transfer providing the temperature distribution through the cell is similar for any outer and inner skin temperature. The conditions for a similar temperature distribution through the cell are (a) the heat capacity of the core is small compared to the heat capacity of the skins, (b) the ratio of heat transfer by conduction to radiation is small or (c) the ratio of heat transfer by radiation to conduction is small.

(4) Additional experimental investigations should be conducted for determining the effective thermal conductivity of both brazed and bonded honeycomb sandwich panels as a function of the average panel temperature for various temperature differences across the panel during conditions of steady state heat transfer.

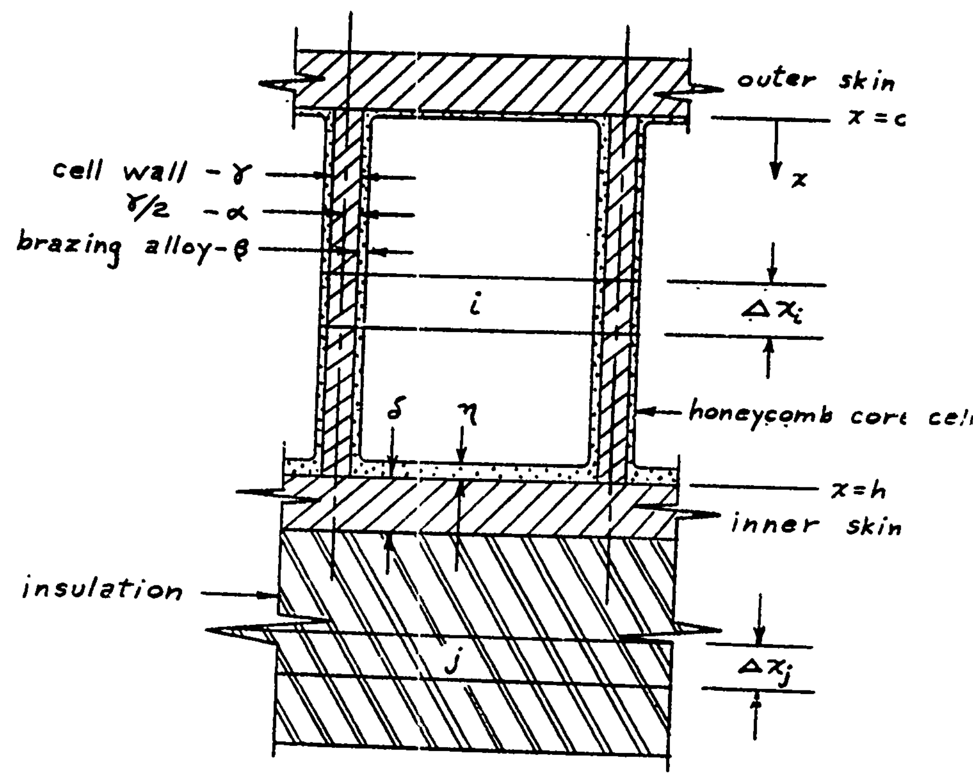

FIGURE 1. BRAZED PANEL HONEYCOMB CORE CELL

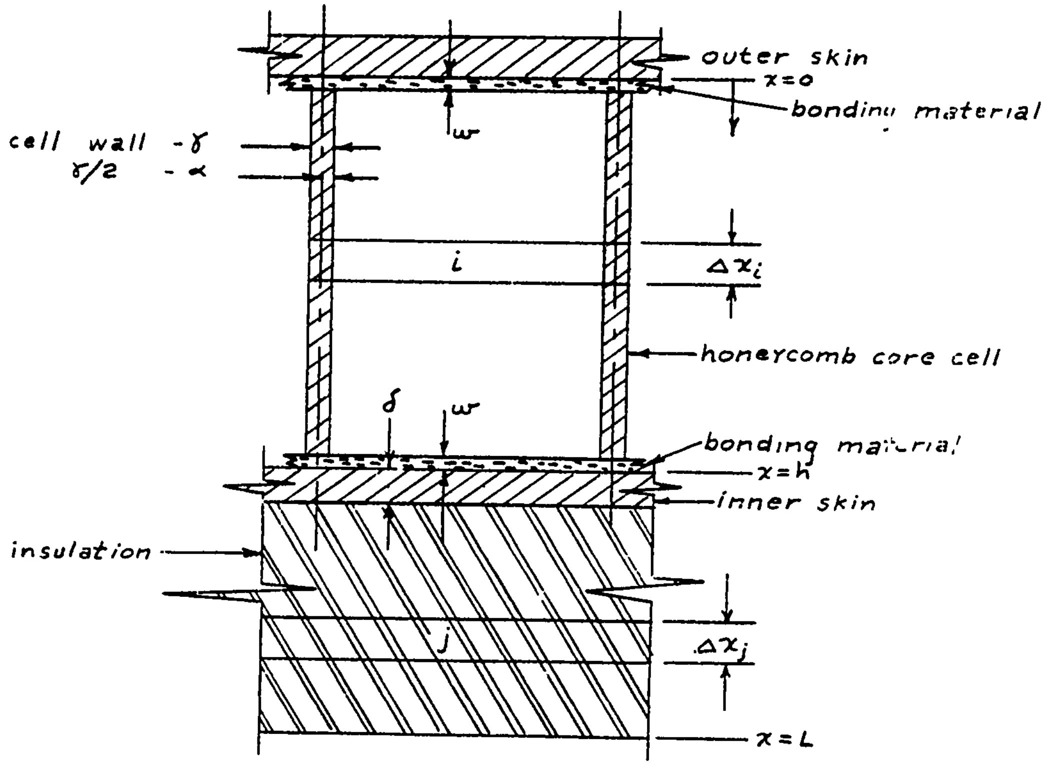

FIGURE 2. BONDED PANEL HONEYCOMB CORE CELL

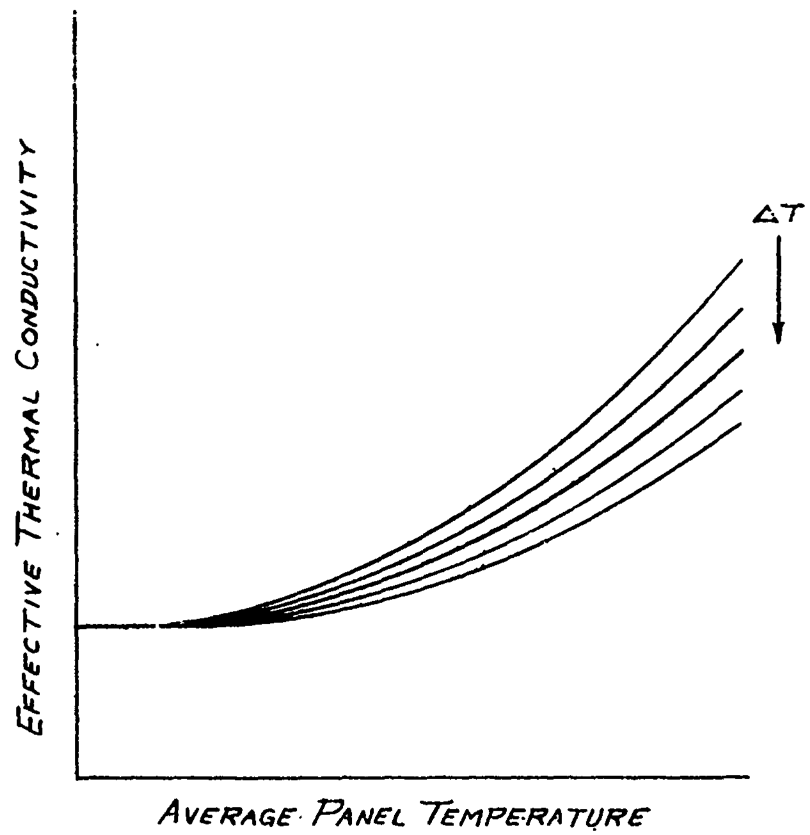

FIGURE 3. EFFECTIVE THERMAL CONDUCTIVITY OF A TYPICAL HONEYCOMB CORE

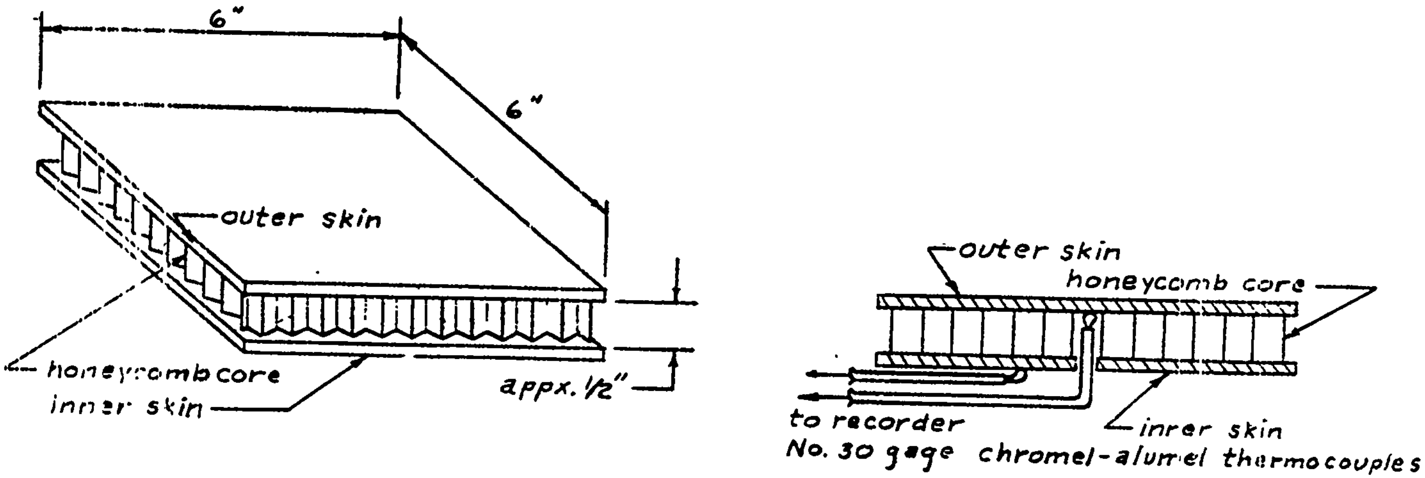

TEST SPECIMEN

THERMOCOUPLE INSTALLATION

FIGURE 4. TYPICAL TEST SPECIMEN AND THERMOCOUPLE INSTALLATION

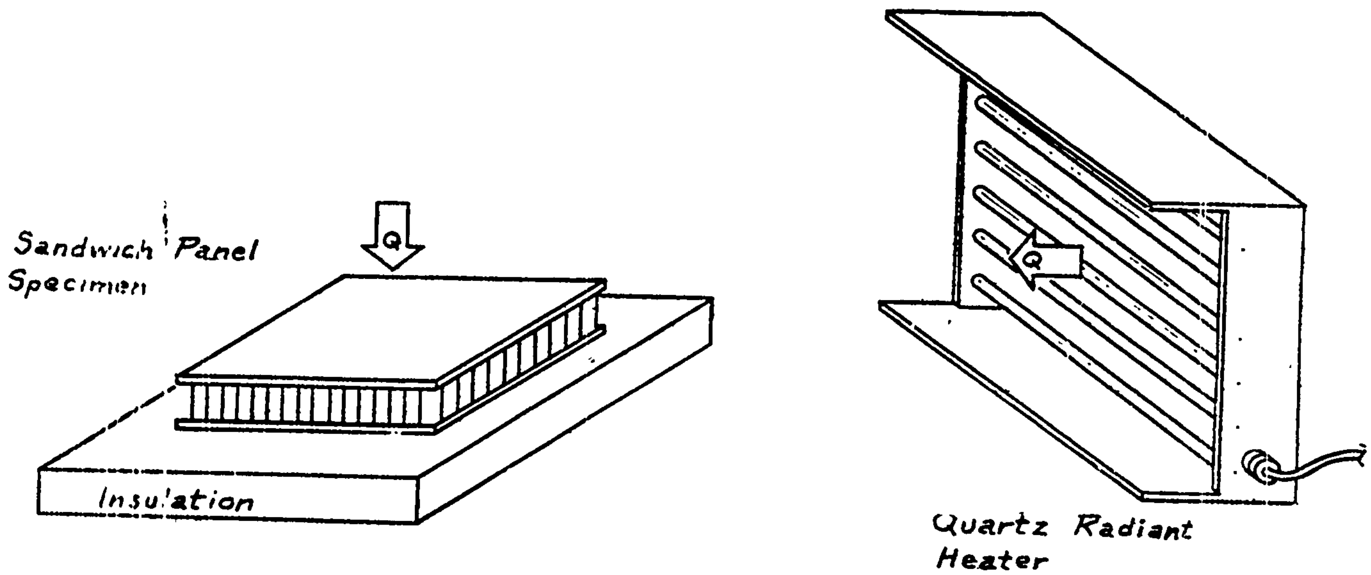

FIGURE 5. TEST APPARATUS

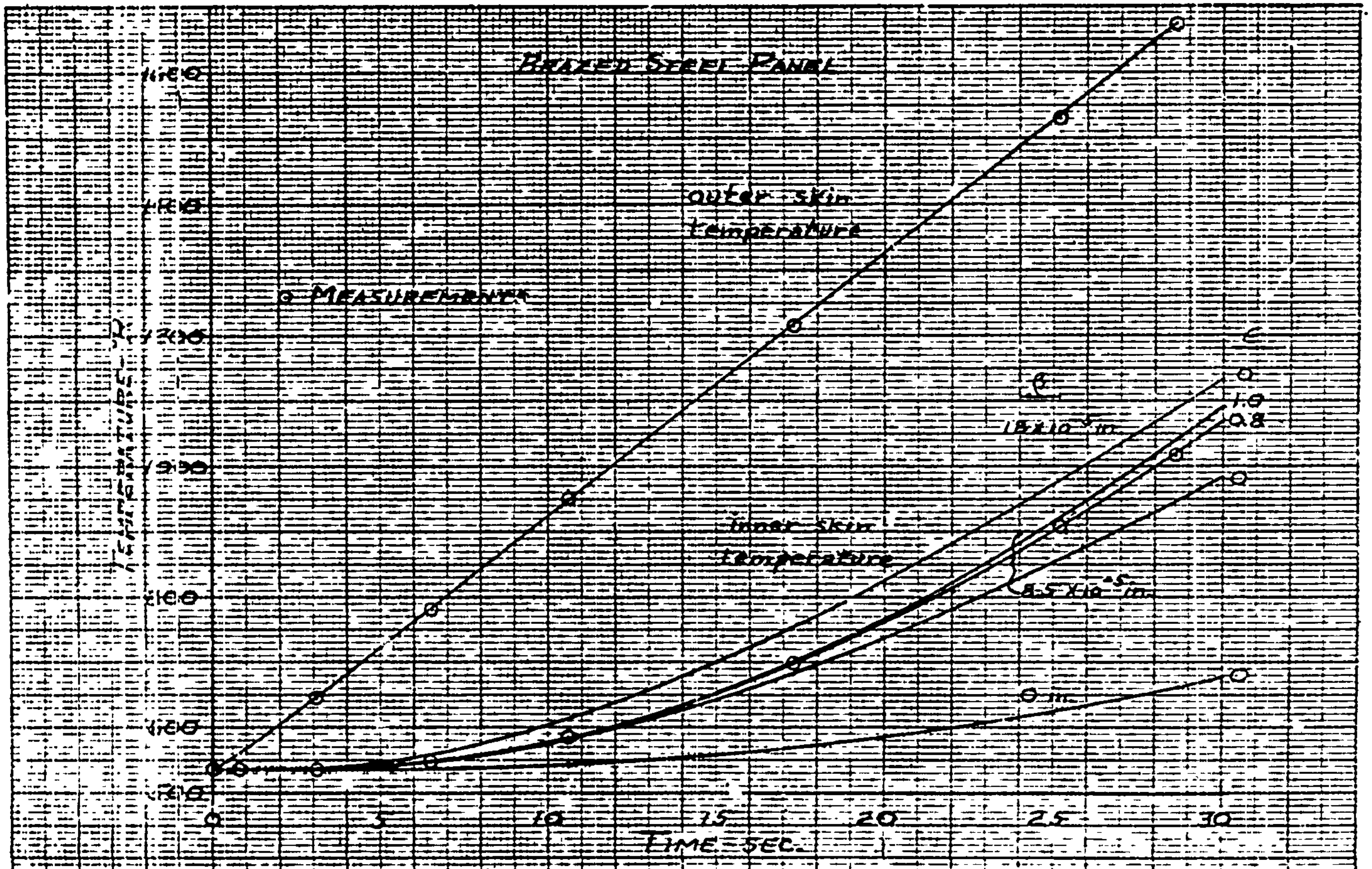

Figure 6. Effects of Brazing Alloy and Cell Wall Emissivity on Inner Skin Temperature

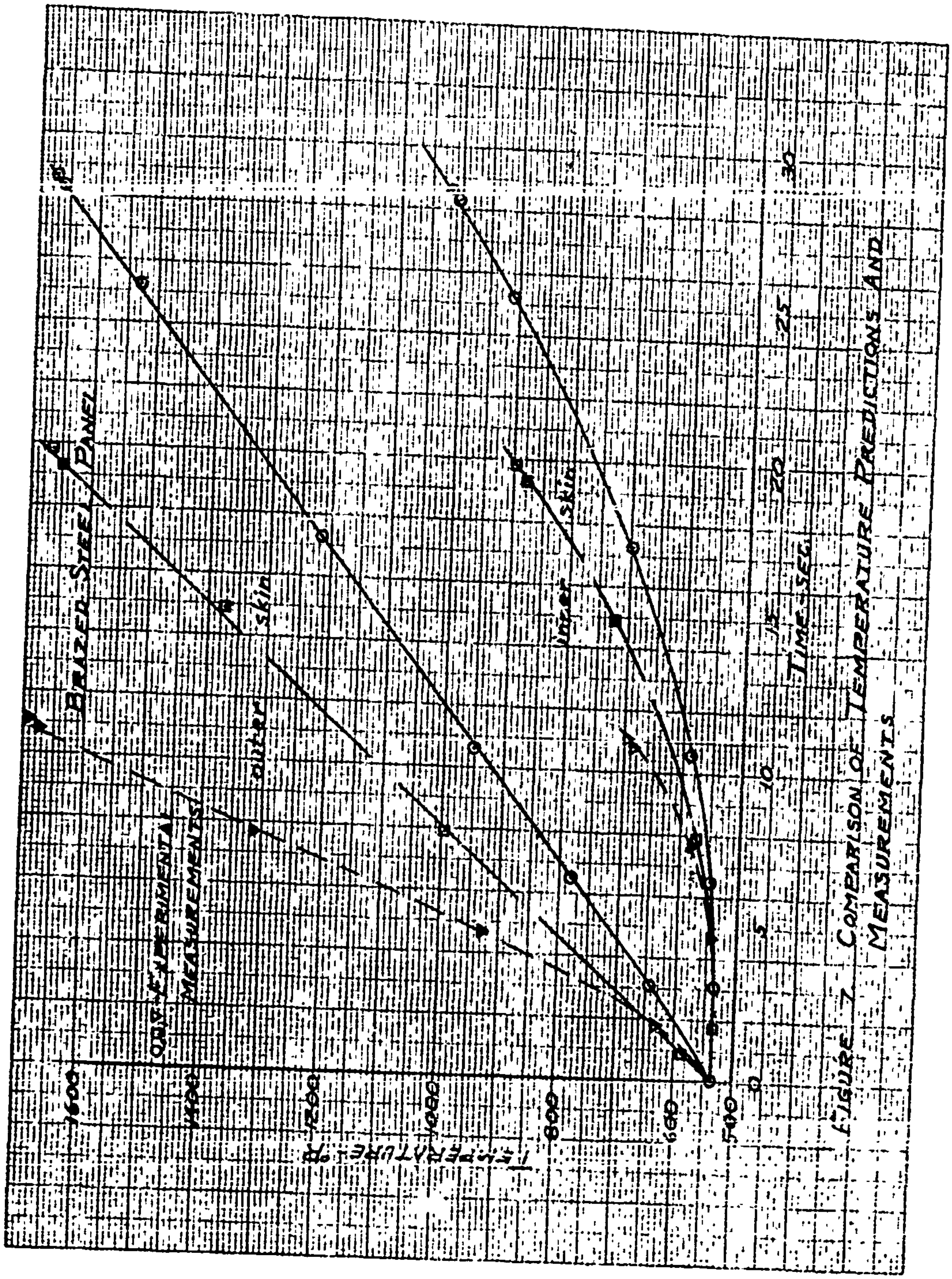

Figure 7 Comparison of Temperature Predictions and Measurements

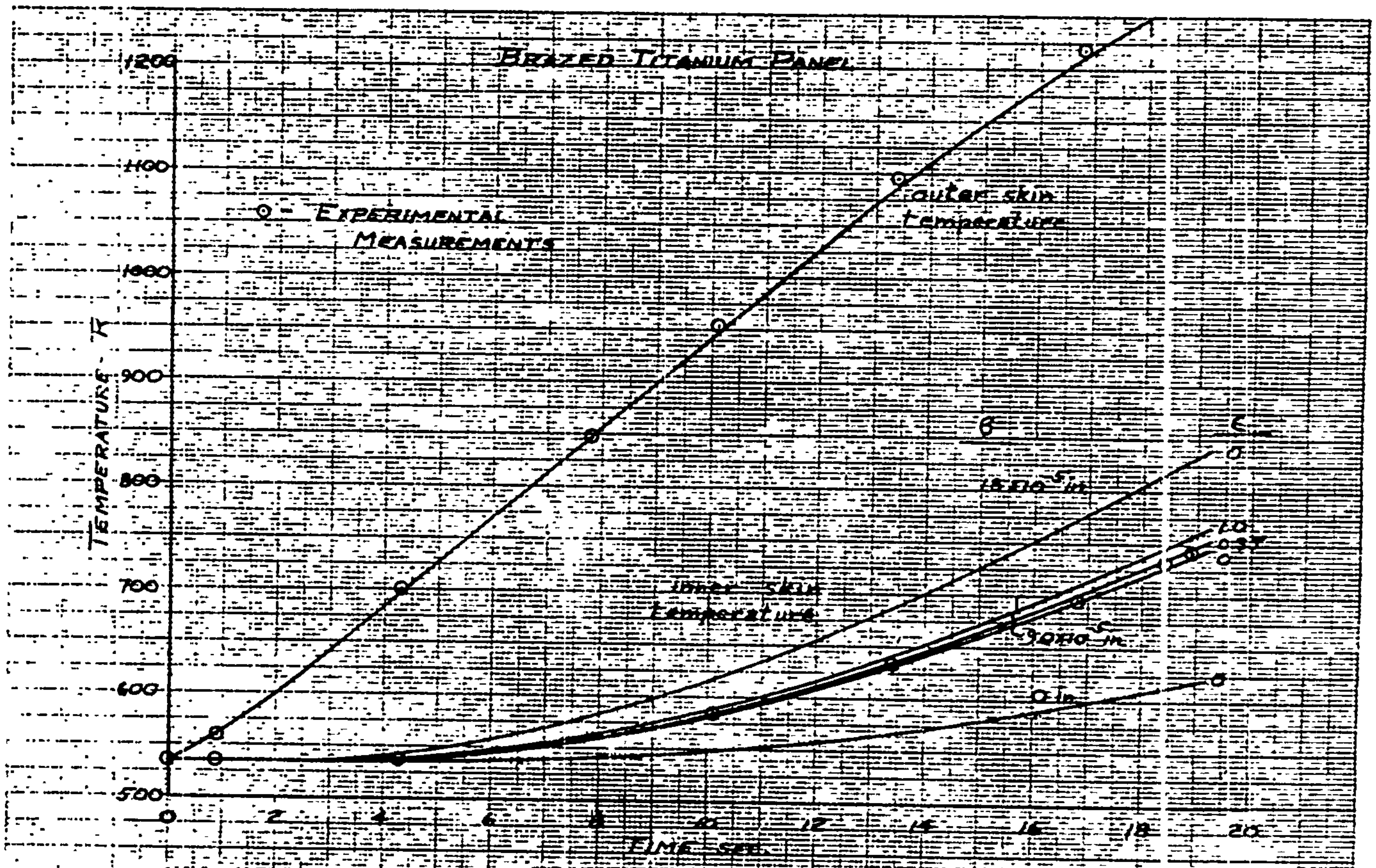

FIGURE 18. EFFECTS OF BRAZING ALLOY AND CELL WALL EMISSIVITY ON INNER SKIN TEMPERATURE

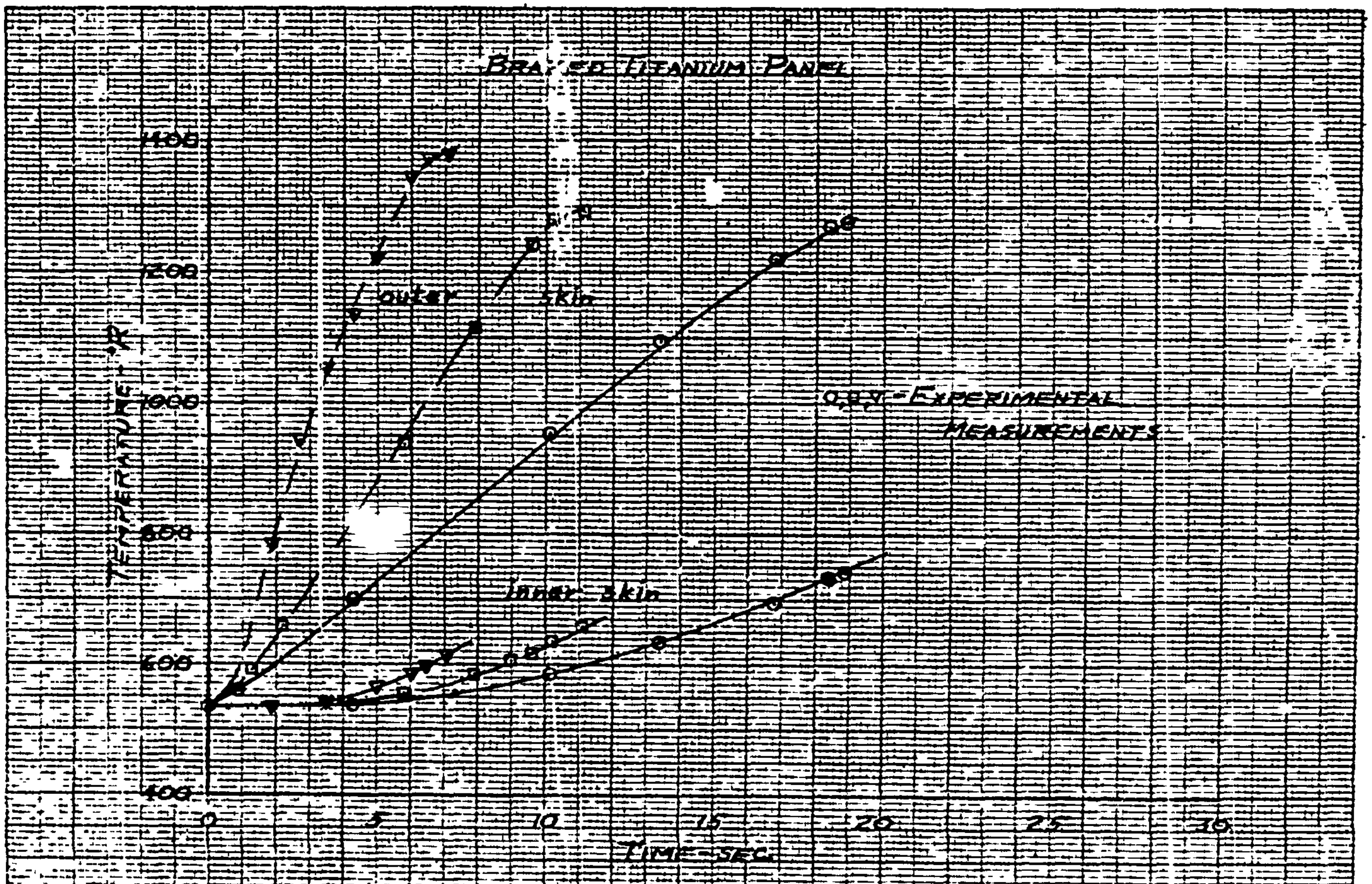

FIGURE 9 COMPARISON OF TEMPERATURE PREDICTIONS AND MEASUREMENTS

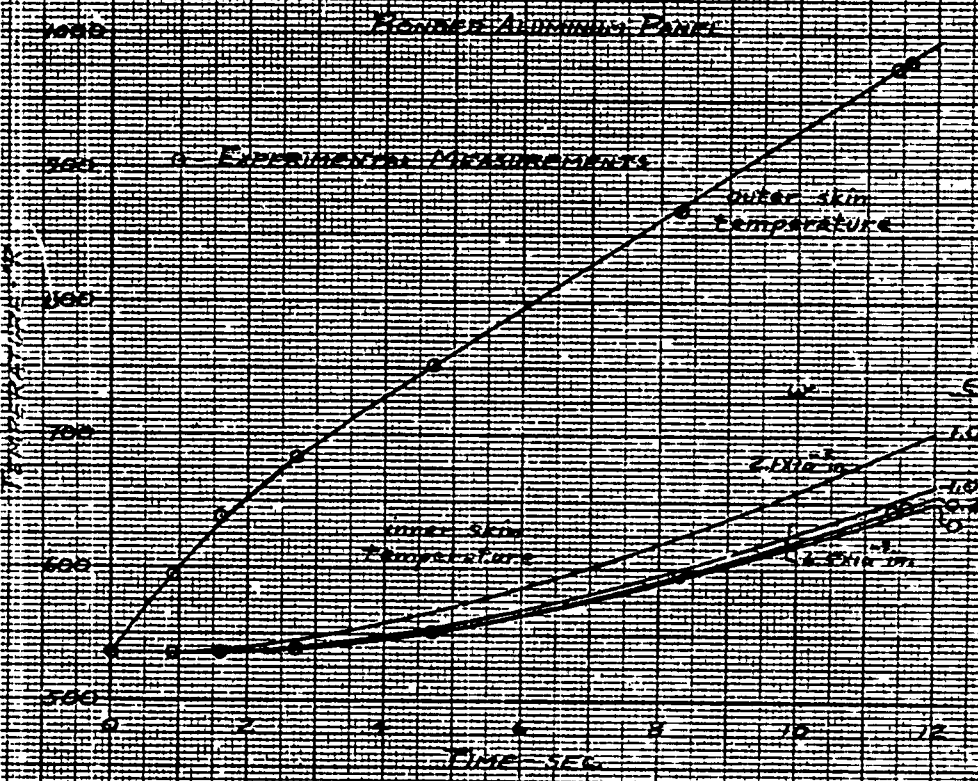

FIGURE 10. EFFECT OF BONDING MATERIAL AND CELL WALL EMISSIVITY ON INNER SKIN TEMPERATURE

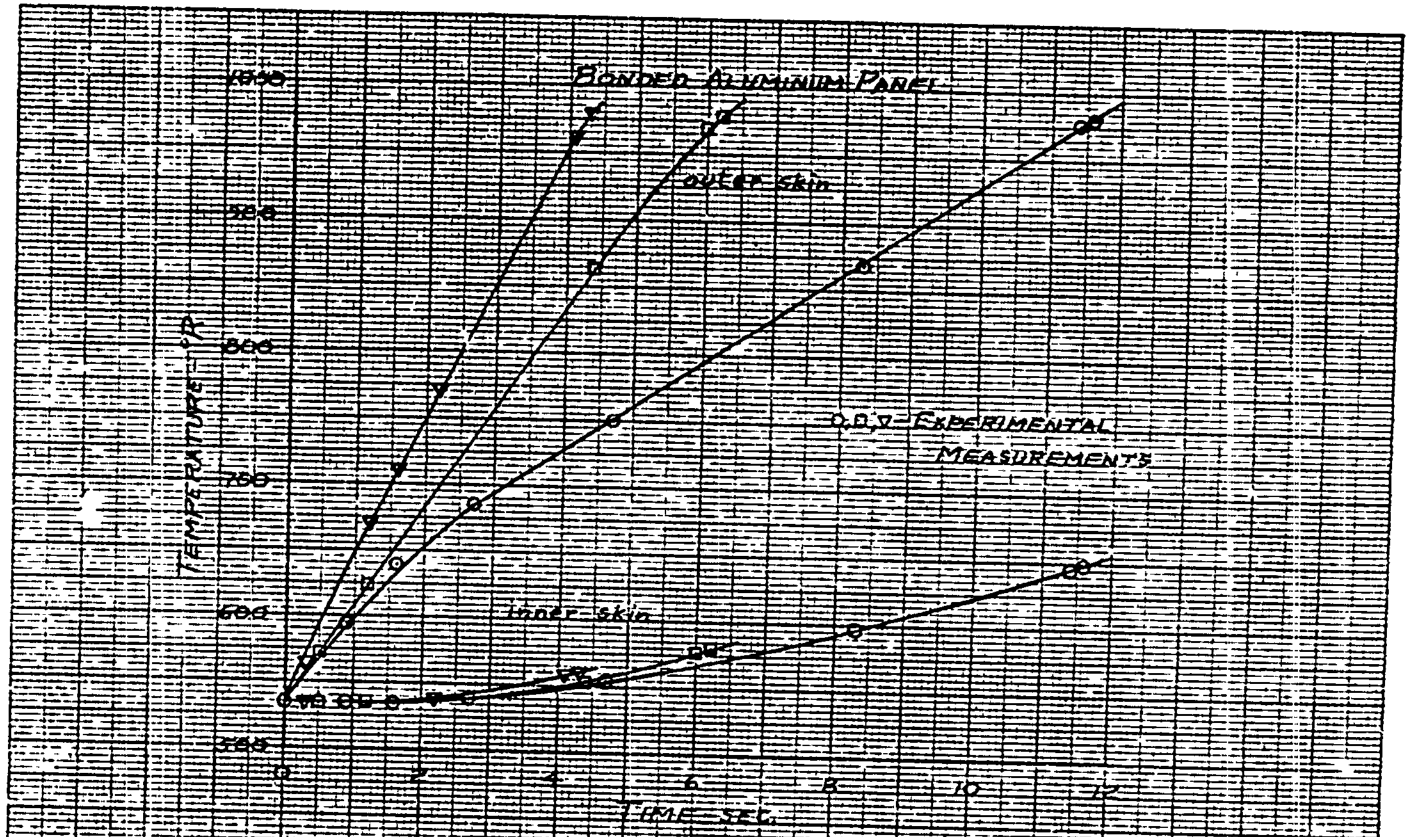

Figure 11. Comparison of Temperature Predictions and Measurements

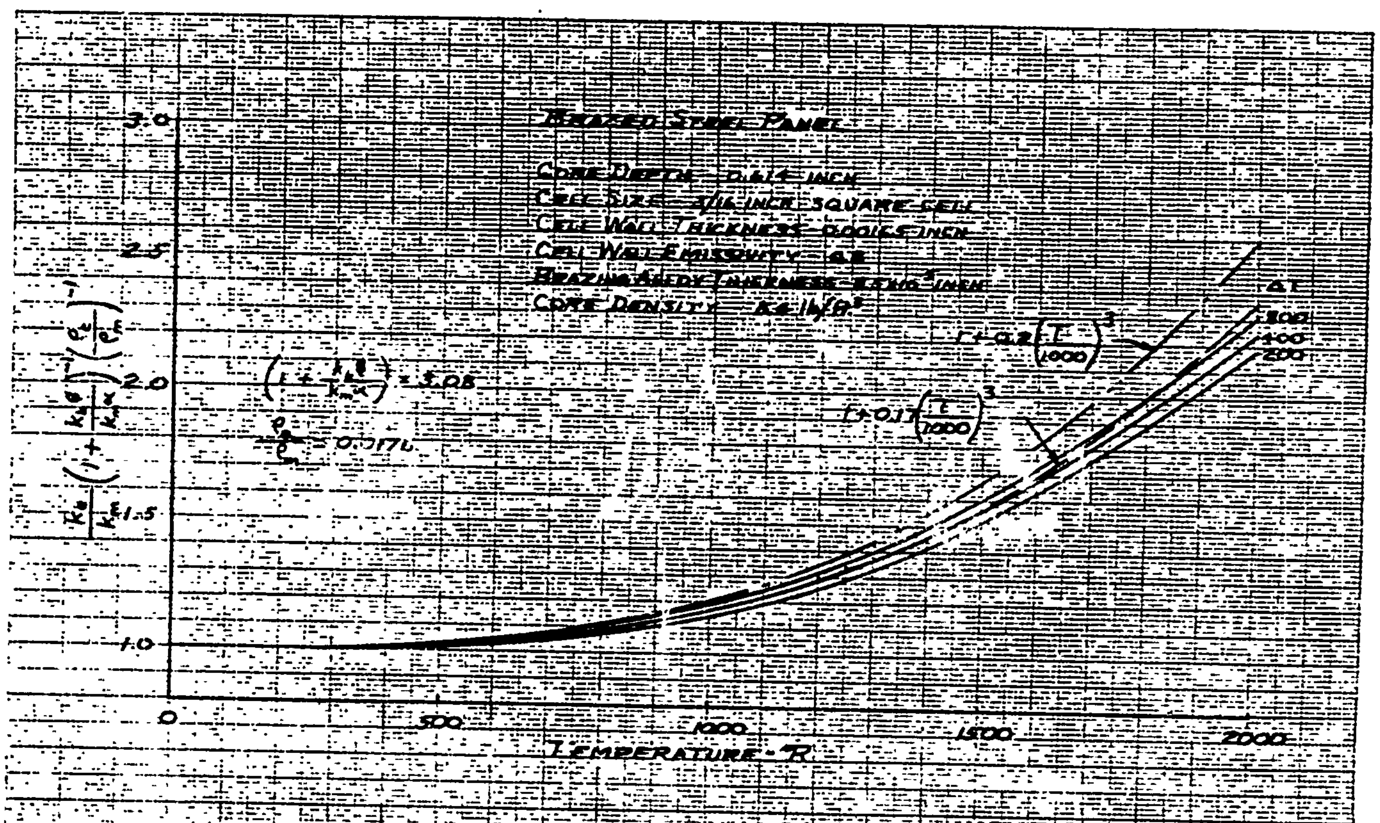

FIGURE 12. EFFECTIVE THERMAL CONDUCTIVITY OF STEEL HONEYCOMB CORE

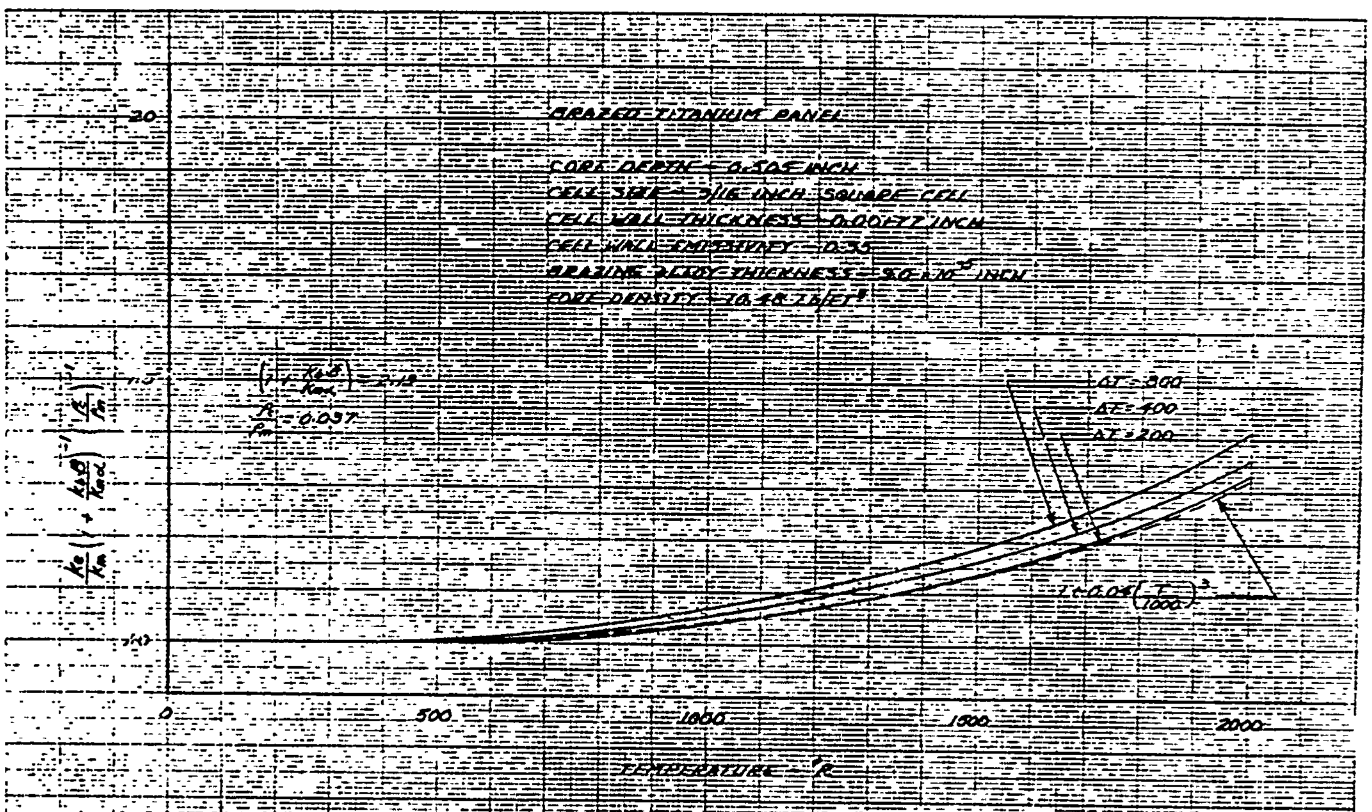

FIGURE 13. EFFECTIVE THERMAL CONDUCTIVITY OF TITANIUM HONEYCOMB CORE